ONERA and SNPE Recent Work on Solid Propellant Combustion Instability

M. BARRÈRE* AND L. NADAUD†
Office National d'Etudes et de Recherches Aérospatiales (ONERA), Chatillon, France
AND
J. N. LHUILLIER‡
Société Nationale des Poudres et Explosifs (SNPE), Paris, France

Results are presented on the response of a solid propellant to pressure and velocity fluctuations. Two different experimental techniques have been developed. The first makes use of devices known to be unstable (L^* or T rocket motors). Comparison of cold and hot tests shows the poor credibility of the results obtained with T rocket motors; furthermore the temperature heterogeneity is scale dependent. In the second technique, research rockets with a modulated throat section are used. These methods are discussed in some detail from the experimental and theoretical standpoints. Here again cold gas comparative tests emphasize the effect of combustion on the observed gain. A linearized theory predicts the observed trends.

Nomenclature

a = sound velocity
b = relative amplitude of the pressure oscillation
c = solid heat capacity
C_p = gas heat capacity
d = relative amplitude of the throat oscillation
h = energy required to transform solid propellant into gases
$\dot{m}$ = mass flow rate
p = pressure
p_e = pressure at nozzle entrance
p_o = stationary chamber pressure
s = Laplace variable
x = exponent in the $v_b = ap^n$ law
u = velocity at the propellant surface
v = velocity
v_b = combustion velocity
v_e = velocity at nozzle entrance
z = abscissa
A = parameter related to the activation energy of the pyrolysis law
A_p = admittance function
A_n = standard nozzle admittance function
A_m = nozzle admittance due to the modulation
B = energetic parameter
C^* = characteristic velocity
L = tube length
L^* = characteristic length
M_b = combustion Mach number
N = frequency
R = propellant response function
S = cross section area
S_b = combustion surface area
S_f = chamber cross sectional area
S_t = throat area
T_{AS} = activation temperature
T_i = initial temperature
T_s = surface temperature
α = amplification coefficient
α_m = growth coefficient
α_d = damping coefficient
γ = heat capacity ratio
ρ = specific mass
τ_f = chamber characteristic time
ϕ = phase shift
ω = fluctuation angular frequency

Presented as Paper 72-1052 at the AIAA/SAE 8th Joint Propulsion Specialist Conference, New Orleans, La., November 29–December 1, 1972; submitted December 19, 1972; revision received July 24, 1973.
Index categories: Combustion Stability, Ignition and Detonation; Fuels and Propellants, Properties of; Solid and Hydrid Rocket Engines.

* Scientific Director, Energetics Department. Member AIAA.
† Research Scientist.
‡ Chief Engineer.

I. Introduction

AT the present time, sufficient information is available to the designer to determine the stationary regime of a rocket motor. However, it is still difficult, in many cases, to forecast the transient regimes. Numerous studies have been devoted to the investigation of combustion instabilities, but it is not yet possible to determine precisely the response function of a propellant and consequently to predict the nonstationary regime.[1]

Determining the range of stable functioning of a rocket motor is therefore a difficult problem. This paper aims at presenting the main results obtained at ONERA and SNPE, which can lead to such a determination. The two techniques described hereafter rest upon the use of either unstable motors, where the instabilities may be started with impulsers, or of motors operating under forced vibrations.

II. Self Sustained Oscillations

The two types of motors used to determine the response function of propellants are L^* and T motors operating in unstable regimes.

L^* Motor (Instabilities of the Nonacoustic Type)

The motor is unstable at low pressures and the observed frequencies are lower than 100 Hz. From the recording of the pressure fluctuations the amplification coefficient, α, can be measured. An elementary theory of this motor shows that the propellant response

$$R = (\tilde{m}/\bar{m})/(\tilde{p}/\bar{p}) = R_r + iR_i$$

is determined by

$$R_r = 1 + \alpha\tau_f \qquad R_i = \omega\tau_f$$

where τ_f is the chamber characteristic time and ω the fluctuation angular frequency. Experimental results show that for most propellants R_r is close to unity in the frequency range investigated. Consequently, this technique is of limited application

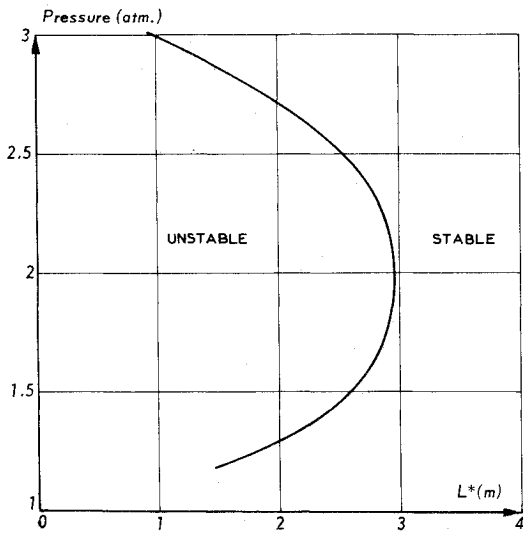

Fig. 1 Stability domain at low frequency (ONERA).

and of little use from a practical viewpoint. Nevertheless, it is possible to determine stability domains such as displayed in Fig. 1. The evolution of the limiting pressure as a function of the characteristic length L^* changes when the nozzle becomes completely subsonic; the domain thus determined is different from that of other workers.

T Burner (Acoustic Type)

In its standard configuration the T burner is made of a cylindrical tube with end burning propellant disks placed at both ends. The gases are exhausted into a large closed tank through an orifice acting as a nozzle and located at the middle of the tube. The apparatus is pressurized with nitrogen to simulate the operating pressures of the chamber.

Instability occurs for many nonaluminized propellants. A system of stationary waves is established in the tube with a frequency $N = \bar{a}/2L$, with L the tube length and $\bar{a}$ the average sound velocity in the chamber. The recorded pressure fluctuations are characterized by the frequency and the amplification coefficients α_m and α_d, for ascending and descending pressures respectively, the evolution being exponential according to an $\exp(\alpha t)$ law. The coefficient α depends upon the gains resulting from the combustion and the different losses. The coefficient α_d, on the other hand, depends only upon the losses (α_d is negative). The parameter $\alpha = \alpha_m + \alpha_d$ is therefore characteristic of the propellant response.

If the admittance function $A_b = \gamma(\tilde{u}/\bar{a})/(\tilde{p}/\bar{p})$ (with $\tilde{u}$ and $\tilde{p}$ evaluated at the propellant surface) is introduced, the propellant response function R is then

$$A_b = \frac{\gamma \bar{u}}{\bar{a}}[R - (\tilde{\rho}/\rho)/(\tilde{p}/\bar{p})]$$

For an isentropic wave the following expression is obtained

$$A_b + \bar{M}_b = \gamma \bar{M}_b R$$

where the Mach number $\bar{M}_b = \bar{u}/\bar{a}$ is the combustion Mach number evaluated at the propellant surface.

A linearized theory applied to this motor shows that the real part of A_b, $A_b^{(r)}$, or R_r, can be evaluated from the knowledge of α

$$\frac{\alpha L}{\bar{a}} = 2(A_b^{(r)} + \bar{M}_b)\frac{S_b}{S_f}$$

where S_b is the area of the combustion surface and S_f the cross-sectional area of the chamber.

Figure 2 shows an example of results obtained at SNPE for a nonmetallized composite propellant of the isolite 30 type

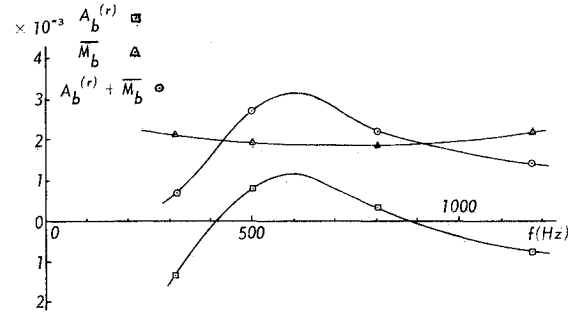

Fig. 2 Acoustic admittance vs frequency, isolite 30 propellant.

(based on ammonium perchlorate and a polyurethane binder). At a pressure of 24 atm (Fig. 2), the admittance goes through a maximum at 600 Hz (and is zero at 400 Hz). For a frequency of 500 Hz, a maximum of the admittance function is observed at 24 atm (Fig. 3). On a radial combustion, star-shaped grain (Mimosa motor), the limiting pressure for the initiation of longitudinal instabilities is 34 atm and the frequency 450 Hz.

In order to enlarge the frequency range, a pulsed T burner has been developed at SNPE, instabilities being set up during combustion by powder impulsers. For propellants containing between 1% and 2% aluminum the motor is stable over the whole frequency and pressure domain, owing to the increase of losses due to alumina. The propellant response is evaluated from the difference between the damping slopes obtained at the time of the impulses during combustion (α_{d1}) and after it has ended (α_{d2}) that is, $\alpha = \alpha_{d1} - \alpha_{d2}$.

Although the T burner technique has greatly progressed and is widely utilized, the results must be used with precaution for the determination of a motor stability. The temperature heterogeneity is such that, when the tube geometry or the burning surface is changed, it should be taken into account for each tube length and therefore for each frequency. Losses are very scale dependent, their effect is partly eliminated by taking the difference between ascending and descending amplitude slopes, but the accuracy remains low.

Without going too much into detail, the results obtained on a T burner without combustion can be cited in order to point

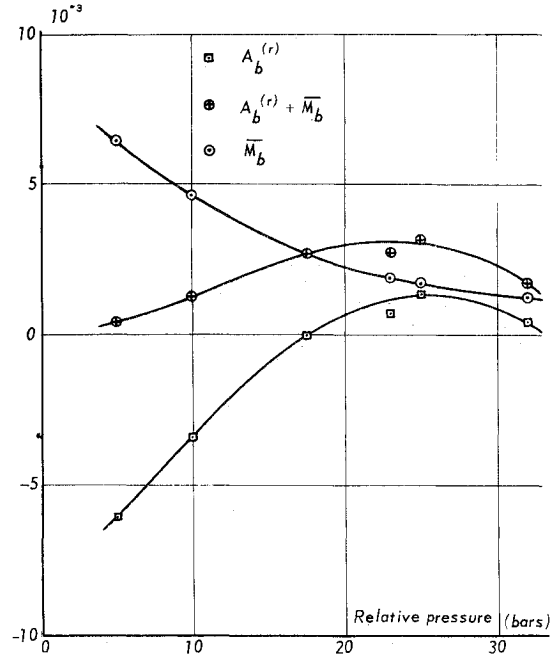

Fig. 3 Acoustic admittance vs pressure.

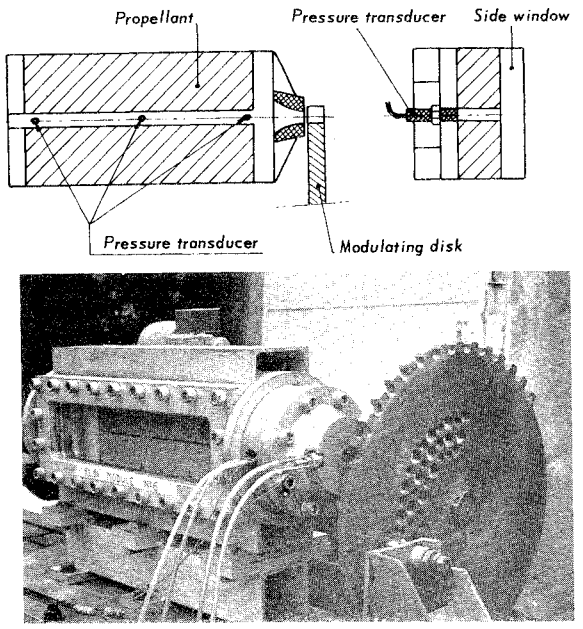

Fig. 4 Schematic arrangement and photography of the burner with side window and modulated exhaust.

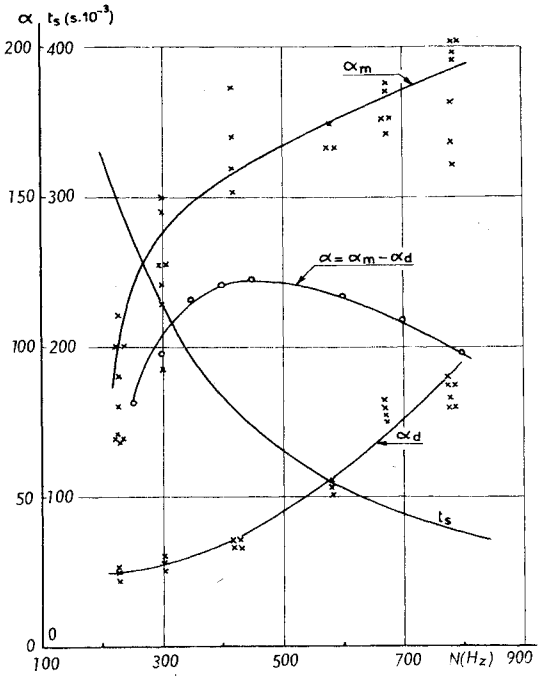

Fig. 5 Results in the case of the T burner with cold gases.

out the errors which can exist when using a T burner to evaluate propellant response.

In the device utilized, nitrogen is fed through a sonic throat at the end of the tube, insuring a constant flow rate, little affected by the pressure fluctuations inside the chamber. The combustion surface was, in some experiments, simulated by a porous plate located close to the nitrogen injection section; the use of this porous plate did not actually change the results and it was removed in some cases. The exhaust of the nitrogen is obtained through two nozzles; one at the other end of the tube, with its section being modulated by a disk (see Fig. 4), the other with a constant section located at mid point between the two ends. The disk has two sectors. The first one modulates the throat area, and at the beginning of this phase an amplification factor, α_m, is recorded. The second one allows the throat to be fully opened and a damping coefficient, α_d, is recorded at the start of this phase. An example of results is shown in Fig. 5. The coefficients α_m and α_d increase with frequency. Generally, the accuracy in the determination of α_m is poorer than for α_d. The results for α_m are very scattered for most of the frequency range. Although there is no combustion, a maximum for $\alpha = \alpha_m - \alpha_d$ is observed for a frequency of 450 Hz.

As mentioned by Buffum, the coefficient α_d decreases when the residence time increases. The empirical relationship offered is

$$\alpha_d = 1.58(aS_t)/(LS_b)$$

where S_t is the throat area, S_b the area of the injection surface simulating the combustion surface, L the tube length, and a the velocity of sound. Since a is proportional to the characteristic velocity C^* and LS_b/S_t represents the characteristic length $L^* = V/S_t$, where V is the tube volume, it follows that $(aS_t)/(LS_b) = kC^*/L^*$ represents the reciprocal of the residence time, t_s, related to the chamber characteristic time τ_f ($\tau_f = t_s/V$ for an isentropic evolution).

The effect of the value of t_s upon the amplification coefficients was also brought to light in the present experiments. Although the variation of α_d vs t_s was found to be in agreement with that of Buffum, a simple relationship $\alpha_d t_s =$ constant was not found. This cold gas experiment points out the difficulties which exist in the interpretation of the results obtained with a T burner.

In our opinion, it is difficult with this technique to properly evaluate the propellant response function; it is nevertheless of great help to obtain an order of magnitude estimate. The use of a pulsed T burner and the comparison of the results with and without combustion could permit an improvement in this method.

Standard Rocket-Motors (Instabilities of the Acoustic Type)

Unstable standard motors can also be used to determine the response function of propellants.

Longitudinal mode

The most important experimental phase corresponds to the study of the longitudinal modes set up by powder impulsers.

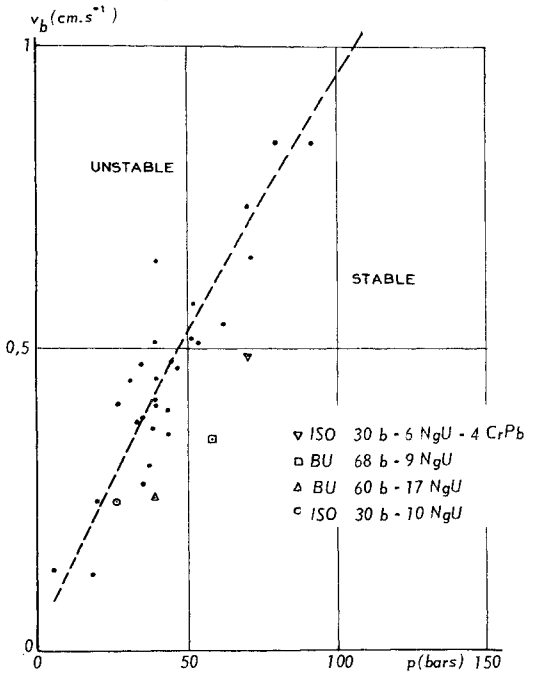

Fig. 6 Longitudinal mode—influence of additives.

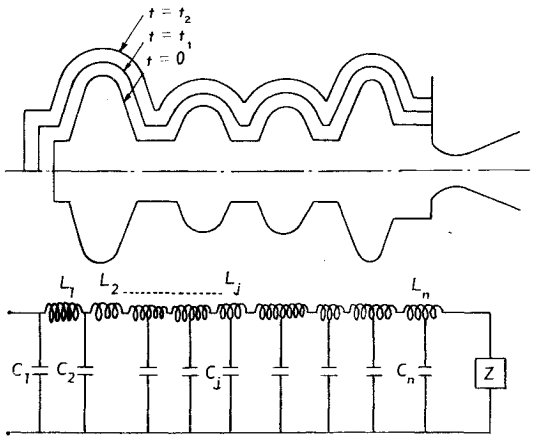

Fig. 7 Longitudinal mode—computation of the frequency.

Most of the results have been obtained on grains with a star shaped cross section, a constant combustion surface and with a 203 mm diam and a 1 m length. This length corresponds to fundamental frequency of about 500 Hz, for which one would expect an important response for the composite propellants used.

During the combustion a black powder impulser, located at the rear end of the motor, is fired to set up an impulse. This impulse leads to a wave train, and if the system is in an unstable configuration, the perturbation is amplified. The limiting pressure for the setting of instability has been determined for a large number of propellant compositions. In the burning velocity-pressure diagram the limiting points are grouped around a straight line which separates stable and unstable domains (Fig. 6). It can be seen that the high combustion velocity propellants are also the most unstable; the influence of additives is related to their action on the combustion velocity. However some additives, such as nitroguanidine, have a stabilizing effect.

The acoustic energy gain being proportional to the area of the combustion surface, it is interesting to determine, for a given instantaneous pressure, the limiting area corresponding to the onset of instabilities. This determination is obtained with a progressive grain (circular cross section, tubular grain).

Tangential mode

The impulse technique has also been used to start up the tangential mode with the aim of studying the damping due to the presence of alumina.

Propellant grain with a nonlinear meridian profile

In order to meet technological requirements, complex geometry grains such as that shown in Fig. 7 are used. The computation of the frequency is more involved. A rough idea of the frequency can be obtained from an analogical computation based on coils and condensers such as displayed in Fig. 7. A more precise method is being developed at ONERA and SNPE, and is based on the use of the wave equations. This method takes into account the boundary conditions in the particular geometry of the grain.

III. Forced Oscillations[2]

With the methods previously discussed, the propellant response function can be determined solely in the domain of unstable operation of the motor. Although the domain of the investigated frequencies is increased by the use of the impulse technique, this domain might not contain that of the instabilities encountered in the application motor. Methods have been developed at ONERA to study the desired frequency range, and particularly the range between 100 and 1000 Hz for which few results are available.

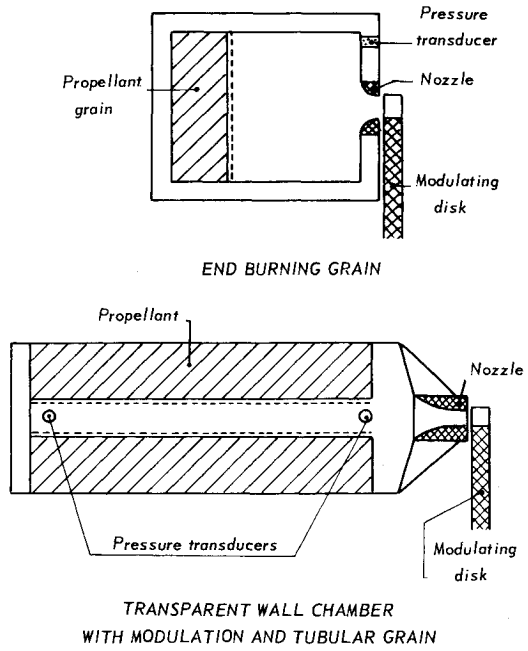

Fig. 8 ONERA burners for the study of combustion instabilities.

The two types of motors which are used are schematically represented in Fig. 8: 1) a chamber with an end burning grain for the study of the burned gas flow-rate-surface pressure fluctuation coupling; and 2) a radial combustion chamber with a combined coupling with pressure and velocity fluctuations along the grain. Pressure and velocity fluctuations are obtained in both cases by modulating the nozzle throat section.

Frontal Combustion Motor, with Modulated Exhaust

The propellant grain is cylindrical with a cigarette combustion; the nozzle is limited to the convergent part and periodic variations of the throat area are obtained with a modulating disk.

A linearized theory describes the operating of the motor and the method is utilized to determine the propellant response function R.

The mass flow-rate through the nozzle is proportional to the throat area S_t, $\dot{m}_t = pS_t/C^*$, and the equation of mass conservation is expressed as

$$\tau_f \frac{d(\tilde{p}/\bar{p})}{dt} = \frac{\tilde{m}}{\bar{m}} - \frac{\tilde{p}}{\bar{p}} - \frac{\tilde{S}_t}{\bar{S}_t}$$

In the case of a sinusoidal throat area modulation following a $\tilde{S}_t/\bar{S}_t = d\exp(i\omega t)$ law, pressure fluctuations are expressed as $\tilde{p}/\bar{p} = b\exp\{i[(\omega - i\alpha)t - \phi]\}$ with a phase shift ϕ between the

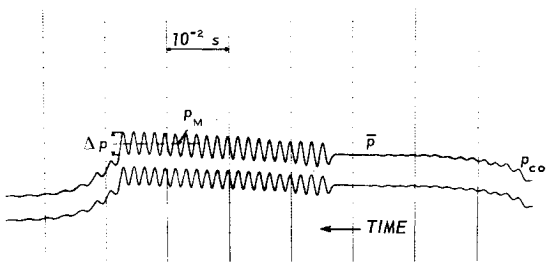

Fig. 9 Recording of the pressure fluctuations for one disk revolution.

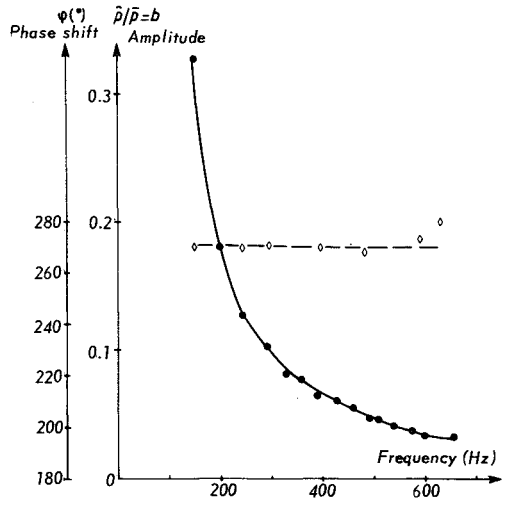

Fig. 10 Variation of the phase shift and amplitude vs frequency.

exhaust modulation and the pressure fluctuation. Introducing into the mass conservation equation the response function R, there results, when $\alpha = 0$,

$$R_r = 1 + (d/b)\cos\phi$$
$$R_i = \tau_f \omega + (d/b)\sin\phi$$

By measuring d, b, $\omega = 2\pi N$ and computing τ_f one can determine R_r and R_i.

The usual modulation procedure is as follows: the disk is divided into three sectors, corresponding respectively to the complete opening of the throat, with a chamber pressure p_o, the half-closing of the throat, with a pressure $\bar{p}$ (the shift from p_o to $\bar{p}$ enables one to obtain a rough estimate of the residence time), and the modulation by the third sector around $\bar{p}$. Figure 9 is a graphic recording of the pressure at two points of the chamber for a frequency around 600 Hz. An example of results is shown on Fig. 10, where the frequency range is from 100 to 700 Hz and where the parameter b is displayed as a function of N. The value of d is close to 0.9. As N increases it is seen that b decreases whereas the phase shift is constant and equal to 270°. As a result, in the domain investigated the real part of R is rather close to unity and reaches 1.6 at 650 Hz. The coupling of $\tilde{m}/\bar{m}$ with the pressure is weak.

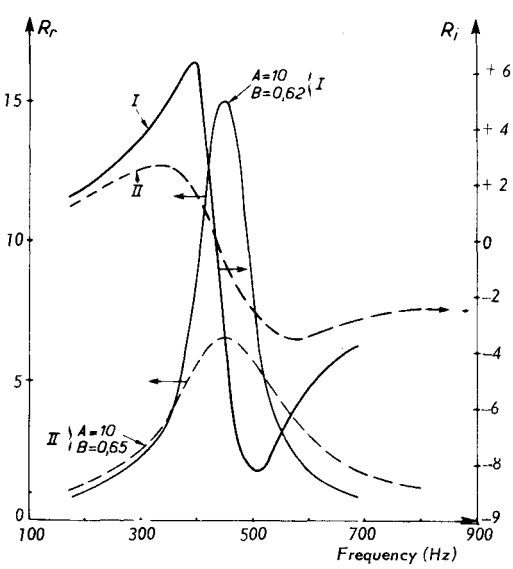

Fig. 11 Variation of R_2 and R_i vs frequency for two response functions $\tau_f = 0.004$s.

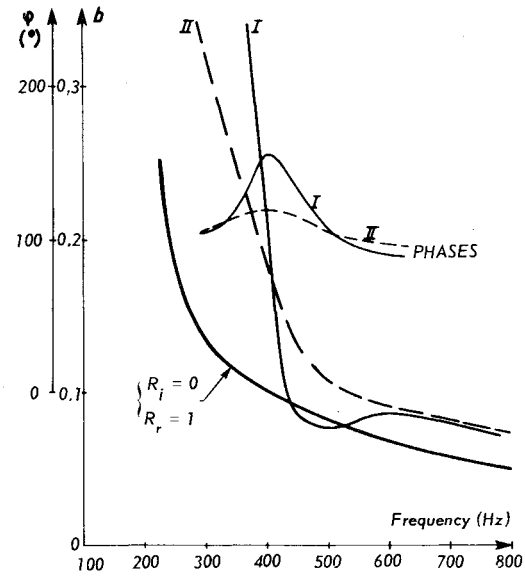

Fig. 12 Variation of the amplitude and phase shift vs frequency for cases I and II.

In order to determine the sensitivity of the method, the theoretical response law obtained from the linearized equations was used

$$R = \left(\frac{\tilde{m}}{\bar{m}}\right)\Big/\left(\frac{\tilde{p}}{\bar{p}}\right) = \frac{nAB + n_s(s-1)}{s + (A/s) - (A+1) + AB} \qquad (1)$$

where n is the pressure exponent which enters into the combustion velocity-pressure relationship, and n_s the pressure exponent which enters into the pyrolysis law. A is related to the activation temperature of the pyrolysis law, $A = (1 - T_i/\bar{T}_s)T_{As}/\bar{T}_s$, with T_i the initial temperature of the propellant and $\bar{T}_s$ the average surface temperature of the propellant. B is a parameter related to the energy Δh required to transform the solid propellant into gases.

$$B \simeq \left(\frac{C_p}{C} - \frac{T_i}{\bar{T}_s} - \frac{\Delta h}{C\bar{T}_s}\right)\Big/(1 - T_i/\bar{T}_s)$$

with C_p the gas heat capacity and C that of the solid. The factor s is the solution of the equation

$$s(s-1) = i\omega\tau_{th} = i\Omega$$

τ_{th} being a characteristic thermal time, ratio of the thermal diffusivity and the squared mean regression velocity of the solid.

Figure 11 displays the variations of R_r and R_i versus frequency for $A = 10$ and two values of B, 0.62 and 0.65, corresponding to a strong and a weak coupling. By inserting these values of R into the results obtained with the linearized theory of the motor it is possible to obtain the values of the amplitude b and the phase shift ϕ. The cases I and II are compared to the case of $R_r = 1$ in Fig. 12. Although changes in the values of b are observed when R_r and R_i vary, the sensitivity of the method is low and depends upon the accuracy of the pressure measurement, mainly at low values of b.

In order to gain a better understanding of the working of this motor, experiments have been carried out with a cold device. The injection of combustion gases from the propellant surface is simulated with the use of a porous plate. The results obtained with this procedure are in agreement with those of the theory, as indicated in Fig. 13.

Radial Combustion Motor with Modulated Exhaust

For the purpose of better approximating the configuration of a standard rocket motor and of avoiding the particular geometry of the T burner, ONERA has developed a two-dimensional chamber with a side window, as shown in Fig. 4.

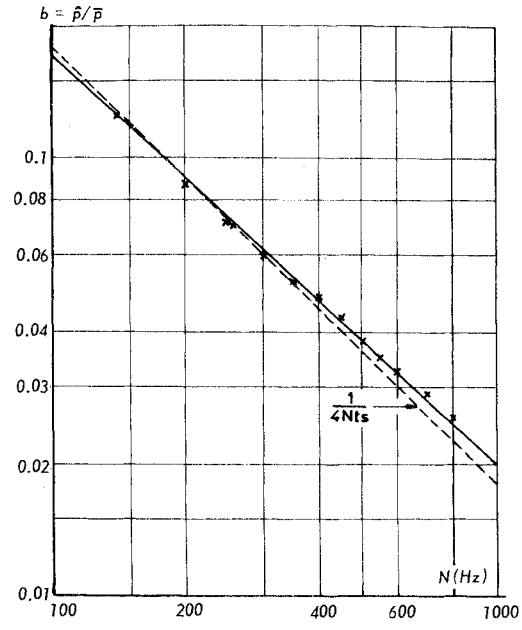

Fig. 13 Variation of the modulation amplitude vs frequency—cold gases.

Two plates, one metallic and the other made of plexiglass, separate two slabs of propellant of rectangular cross section, between which the burned gases can flow. On the front end the chamber is limited by a plate and on the rear end an axisymmetric nozzle is affixed; an intermediate chamber forms a transition from the rectangular chamber to the circular section of the nozzle. At the exit of the throat a rotating disk modulates its area.

Two flush membrane pressure transducers are located at each end of the grain. This device is well adapted to the investigation of intermediate frequencies with the possibility of a coupling at the propellant surface between burned flow rate and pressure and velocity fluctuations. The disk, as before, is designed for three successive phases: full opening, half opening and modulation of the throat. During one rotation of the disk it can be assumed that the modulation frequency as well as the chamber characteristic time, are constant, so that one rotation permits one to obtain one measurement point. During a single firing it is possible to scan a frequency range by varying the disk rotation velocity.

The results obtained for one propellant are displayed in Fig. 14, where it is seen that the pressure fluctuation amplitude changes differently, depending upon the transducer location. A resonance frequency at 700 Hz is found, corresponding to the chamber fundamental longitudinal mode. The amplitudes at the forward end are more important than at the nozzle entrance and at resonance the ratio is about 2. At the forward end an increase in amplitude is seen between 200 and 400 Hz, pointing out to a pressure coupling more important than the velocity coupling. The differences obtained between the two transducers can be assigned to the differences in the flow conditions as well as in the structure of the combustion zone. The phase shift between the two signals (also shown in Fig. 14) increases with frequency and goes through 180° at resonance, corresponding to a tube resonating in $\lambda/2$.

High speed films show a periodic structure of the combustion zone. The perturbation is felt all along the tube and it would not be appropriate to introduce a threshold velocity v_o equal to that used for the permanent regime law. The influence of the velocity v, in evolution along the surface, is proportional to the difference

$$\{|\tilde{v}+\bar{v}-v_o|-|\bar{v}-v_o|\}$$

where $\bar{v}$ is the average velocity along the grain.

Again, in order to have an appropriate reference, experiments without combustion were performed with a cold device. In this case the two pressure transducers indicate the same variation of the relative amplitude $\tilde{p}/p$ as a function of frequency, with a tube length chosen so as to have the same resonance frequency, ~700 Hz (Fig. 15). By comparing the curves of Figs. 14 and 15 one can obtain an estimate of the changes brought about by the combustion process. An investigation of this motor with the help of a linearized theory explains these differences.

Before looking into the description of the chamber flow phenomena, it is necessary to determine the nozzle transfer function. The throat area oscillation, of amplitude d and frequency ω, leads to pressure and velocity oscillations, $\tilde{p}_e$ and $\tilde{v}_e$, of the same frequency at the entrance of the nozzle. The physical condition requiring that the flow is sonic at the throat implies a relationship between the three quantities d, $\tilde{v}_e$, and $\tilde{p}_e$, a relationship which is the boundary condition imposed on the chamber flow by the nozzle.[3] For the sake of keeping the simplicity which corresponds to the one-dimensional computation, the model of the nozzle flow represented in Fig. 16 is employed. The nozzle is considered as a one-dimensional convergent, with oscillating walls over the whole length. At a given abscissa z of the nozzle, the cross-sectional area is given by

$$S = \bar{S}(z)[1+\alpha'(z)\,e^{i\omega t}]$$

The velocity, pressure and specific mass are given by

$$v = \bar{v}(1+v'\,e^{i\omega t}),\quad p = \bar{p}(1+\gamma\eta'\,e^{i\omega t}),\quad \rho = \bar{\rho}(1+\sigma'\,e^{i\omega t})$$

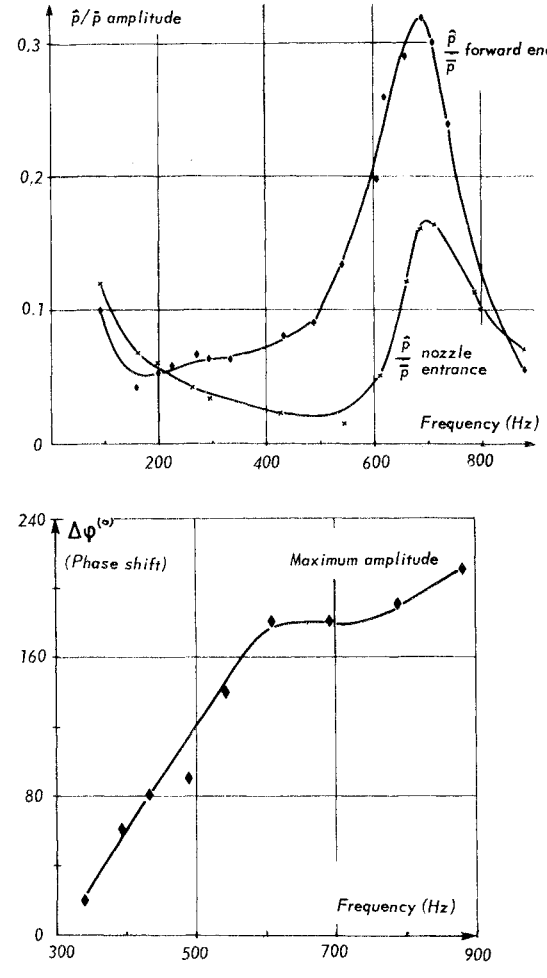

Fig. 14 Amplitude vs modulation frequency ($p = 33$ bars). Phase shift between the two pressure transducers versus frequency—tubular grain.

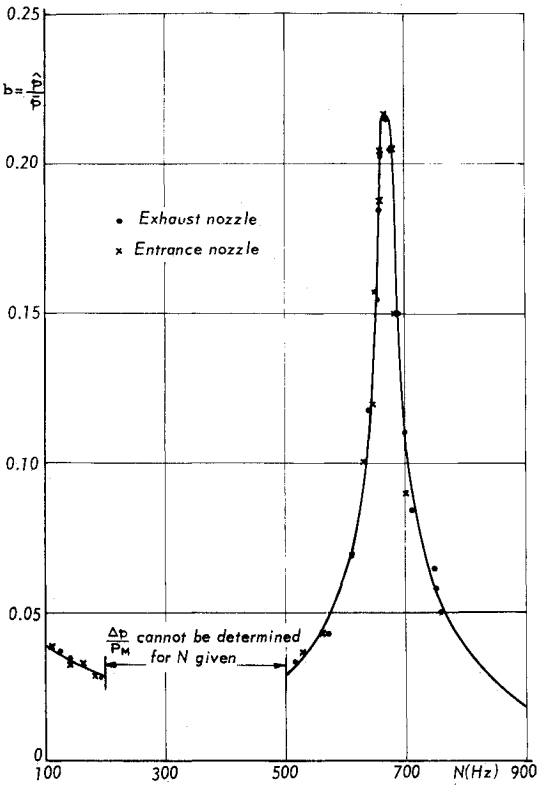

Fig. 15 Amplitude vs frequency—cold gases.

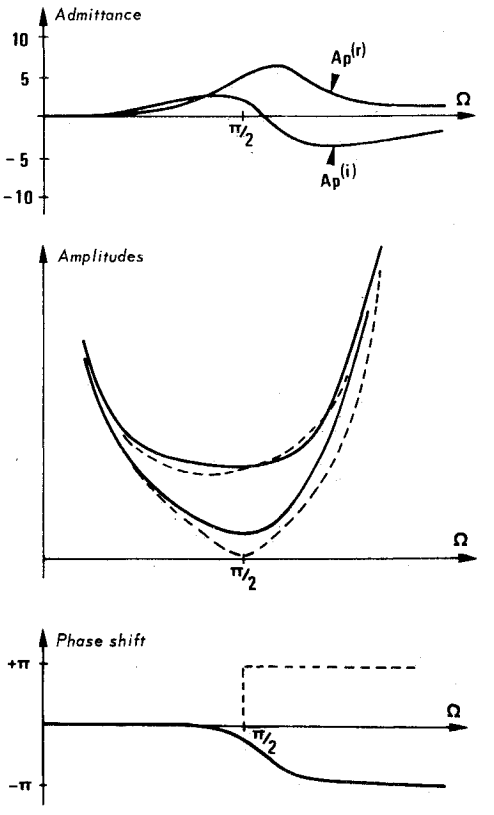

Fig. 17 Admittance, amplitude, and phase shift.

If an isentropic evolution in the nozzle is assumed, $\sigma' = \gamma\eta'$. It is assumed furthermore that, for a conveniently chosen origin of the abcissae, $\bar{v}$ is proportional to z, from which it follows that

$$\frac{\bar{v}_e}{z_e} = \frac{\bar{v}}{z} = \frac{\bar{a}^*}{z^*} = \frac{\bar{a}^* - \bar{v}_e}{\lambda}$$

the index star designates the throat conditions and λ the nozzle length. With the new variables $x = z^2/{z_*}^2 = \bar{v}^2/{a_*}^2$ and $\beta = \omega z_*/\bar{a}_*$, $\beta = \lambda\omega/(\bar{a}_* - \bar{v}_e)$, a nonhomogeneous hypergeometric equation is obtained for η', to which must be added the regularity condition at $x = 1$, corresponding to a sonic throat.

α' is assumed to vary linearly with x, $\alpha' = (x - x_e)d/(1 - x_e)$. At $x = x_e$ the linearized transfer function is obtained in the form

$$v_e' = A_n\eta_e' + A_m d$$

A_n is the standard nozzle admittance function, as given by Crocco.[4] The quantity $A_m d$ corresponds to the contribution to the nozzle entrance velocity oscillation due to the throat modulation

$$A_m = \frac{(\gamma+1)(4+i\beta)}{4(\gamma+1)+6i\beta-\beta^2}$$

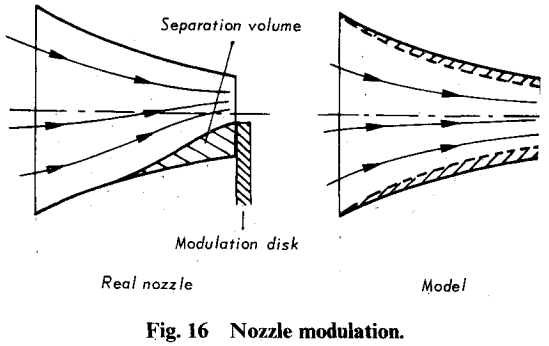

Fig. 16 Nozzle modulation.

If one takes as the propellant response function the expression of Eq. (1), and assumes that the combustion process is sensitive to the pressure oscillations as well as to the velocity oscillations at the surface of the propellant, the following results are obtained.

The combustion velocity fluctuation is taken as $v_b'/\bar{v}_b = A_p\eta' + A_v M'$, $(v_b = \dot{m}/\rho_p)$ where A_p and A_v represent the contributions from the pressure and the velocity and M' is the fluctuation Mach number, $v'/\bar{a}$; the additivity of the two effects is in agreement with the linearization scheme. Two cases have been investigated depending on whether or not the coupling is strong. The investigated domain has been divided into three frequency ranges, low, intermediate, and that around the characteristic frequency of the chamber.

For the low frequencies the solution is particularly simple

$$\eta' = A_m d/(A_n - A_p)$$

For these frequencies, the oscillations in the whole chamber are in phase with an amplitude of the order of that of the throat modulation. It should be mentioned that the pressure coupling enters significantly, whereas the velocity coupling disappears. This result is analogous to that obtained with the frontal combustion motor.

For the intermediate frequencies and a weak coupling (A_p and A_v of the order of 1), the amplitude of the oscillations depends weakly upon the propellant response. An important coupling, on the other hand, does not lead necessarily to high amplitude oscillations; they remain of the order of $\bar{M}_e d$ (with $\bar{M}_e$ the Mach number at the entrance of the nozzle).

In the frequency range close to the chamber characteristic frequency, both pressure and velocity couplings affect the oscillation amplitude.

Figure 17 shows an example where the chosen admittance function is displayed on the upper graph; the pressure amplitudes at the forward end and nozzle entrance are shown on the middle graph, the arrangement of the curves corresponding to that of the experiment (Fig. 14). The phase shift between the forward end and the nozzle entrance is indicated on the lowest graph. In these figures the dotted lines correspond to a null

coupling and the full lines to the strong coupling of the upper graph.

In conclusion, the amplitudes at the forward end are higher than those at the nozzle entrance, in phase for the low frequencies, out of phase for the higher frequencies. The amplitudes tend to equalize each other at the very low frequencies. At the resonance frequency the experimental results show an important difference between the two amplitudes, and for which the linearized theory cannot yet account.

IV. Conclusion

In France, investigation of solid propellant combustion instabilities is performed both with the help of standard methods, utilizing unstable motors, and of forced oscillation methods. The L^* motor operates only at low pressures and in a narrow frequency range; the use of this technique is consequently limited.

The T burner provides results which are difficult to interpret, as pointed out by the information obtained with the device operating with cold gases. It is an appropriate tool to estimate the order of magnitude of the propellant response function; however, no great accuracy can be expected. The pulsed T burner, proposed by Price in the United States, is an important improvement since it allows one to increase the frequency domain being investigated and to obtain the response function with better accuracy.

The coupling of the burned mass flow rate fluctuation to that of the pressure can be investigated fairly simply with the use of the frontal combustion, modulated exhaust motor. The comparison of the results obtained with cold gases are in good agreement with the theoretical model.

The interpretation of the experiments is simple and one can use, as a first approximation, the simplified formulas proposed for the response function. The precise knowledge of its real and imaginary parts enables the calculation of the parameter A, related to the kinetics of the propellant pyrolysis, and the energetics parameter B[2], as well as to improve the theory.

In addition to the simplification in the interpretation of the experimental results, the frontal combustion, modulated exhaust device offers the following advantages: the experiments are carried out in conditions close to the real ones, and identical for all frequencies since the apparatus remains the same. The energy losses are low.

The propellant response function can be obtained with a limited number of experiments. The radial combustion, modulated exhaust motor, closer to the real configuration, is such that the propellant undergoes pressure as well as velocity fluctuations.

The comparison of the results obtained with cold gases and with combustion gases shows the sensitivity of the method. Furthermore, changes in the combustion phenomena and in the average local combustion velocity with the oscillation frequency can be investigated. The interpretation of the experimental results with the help of a linearized theory is more difficult than in the case of the frontal combustion device. In the low frequency domain, only the effect of the pressure coupling remains. In the intermediate frequency domain, in the case of a moderate coupling, the pressure amplitude is little affected by the propellant response. This amplitude changes when the coupling is strong, although its order of magnitude remains the same. Methods utilizing a modulated exhaust motor permit an improvement in the experimental investigation of solid propellant longitudinal instabilities.

In the case of the frontal combustion device it appears fairly easy to improve the method, from the experimental as well as from the theoretical viewpoints. This improvement will be more difficult for the theoretical description of the radial combustion device.

References

[1] Williams, F. A., Barrère, M., Huang, C., "Fundamental Aspects of Solid Propellant Rockets," AGARDograph 116, 1969, pp. 555–673.

[2] Barrère, M., Nadaud, L., "Prévision des Domaines de Fonctionnement Instable d'un Propulseur à Propergol Solide," *22nd International Astronautical Congress*, Brussels 1971; also *Astronautical Research 1971*, Reidel Publishing Company, Brussels 1973, pp. 265–289.

[3] Debout, B., "Théorie Linéaire d'un Propulseur à Propergol Solide à Ejection Modulée," *23rd International Astronautical Congress*, Vienna 1972.

[4] Crocco, L. and Cheng, S. I., "Theory of Combustion Instability in Liquid Propellant Rocket," AGARDograph 8, 1956, p. 197.